

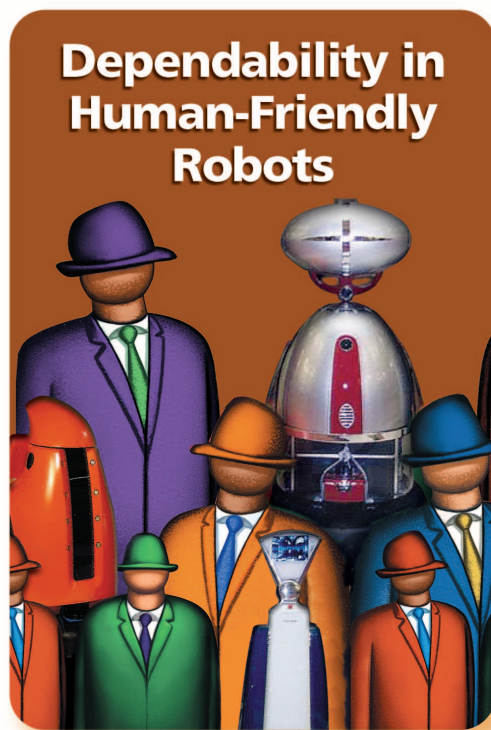
*Dealing with the Safety-Performance Tradeoff  
in Robot Arms Design and Control*

# Fast and “Soft-Arm” Tactics

By ANTONIO BICCHI and GIOVANNI TONIETTI

A robot arm that is to interact with humans has a single design consideration at a premium—safety. Under no circumstances should the robot arm cause harm to people in its surroundings, directly or indirectly, in regular operation or in failures. Having stated this, the second most crucial requirement for robot manipulators is their accuracy and rapidity in performing tasks when required. This article reports on different possible approaches for dealing with the problem of achieving the best performance, under the condition that safety is guaranteed throughout task execution.

Robot safety involves several different considerations and depends on many factors, ranging from software dependability, to possible mechanical failures, to human errors in interfacing with the machine, etc. A thorough hazard analysis and risk evaluation should be performed according to methodical procedures specifically for different domains of application: these methods are receiving growing attention from both the scientific community (e.g., [1]–[3]) and international standardization bodies (see, for instance, [4]). General hazard management considerations are very broad, of course, and fall beyond the scope of this article. Here, we will only consider a specific, if very important, type of risk: the situation in which, in an unspeci-



fied instant during execution of a preplanned robot arm movement, a collision between a link of the arm and a human occurs. The quantitative analysis of the trade-off between such risk and the performance obtainable is one of the objectives of our work. Such analysis has a strong impact on how robot mechanisms and controllers should be designed for human-interactive applications, giving rise to a paradigm shift in robot design, which we will examine in detail.

### **Previous Work**

Robots designed to share an environment with humans, e.g., in domestic, entertainment, assistive, rehabilitation, or medical applications [5]–[8], must fulfill different

requirements from those typically met in industry. It is often the case, for instance, that absolute accuracy requirements are less demanding. On the other hand, a concern of paramount importance is safety and dependability [1], [3] of the robot system. According to such difference in requirements, it can be expected that usage of conventional industrial arms for anthropic environments is far from optimal.

The inherent danger to humans of conventional arms can be mitigated by drastically increasing their sensorization (using proximity-sensitive skins such as those proposed in [9] and [10], for example) and/or by modifying their controllers.

Active stiffness and impedance control could be employed to introduce compliance with respect to sensed interactions. However, these approaches may not prove robust with respect to impacts on portions of the arm that are not equipped with sensors. Also, it is well known in the robotics literature that there are intrinsic limitations to what the controller can do to alter the behavior of the arm if the mechanical bandwidth (basically dictated by mechanism inertia and friction) is not matched to the task (see, for example, [11]). In other words, making a rigid, heavy robot to behave gently and safely is an almost hopeless task if realistic conditions are taken into account. Probably the first lightweight arm for service applications was the whole-arm manipulator (WAM), proposed by [11]. The stress on safety has pushed a number of technological innovations in actuators, sensors, and structural design in recent years, leading to impressive realizations such as the generation of DLR lightweight robots [12]. Arms in this class are primarily characterized by the low inertia of their links and by backdrivability. A relatively small amount of joint compliance is often present in these arms as a side-effect of other design choices such as cable transmission or joint torque sensors. Suitable force-control policies have been designed to employ such arms in safety-critical applications [13]–[15].

Another approach to increasing the safety level of robot arms interacting with humans is to intentionally introduce mechanical compliance in the design. By this measure, which is still, of course, to be accompanied with low-inertia design of the arm's links, researchers tend to dynamically decouple the actuator's rotor inertia from the links whenever an impact occurs. Naturally, compliant transmission can negatively affect performance in terms of increased oscillations and settling time. Accuracy in positioning and stiffness tuning should then be recovered by suitable control policies.

In this article, we first provide a discussion of the intrinsic limits of performance imposed by safety constraints. The achievable trade-off is illustrated with several joint actuation examples, including a rigid transmission, a passive elastic joint, the distributed macro-mini (DM<sup>2</sup>) actuation scheme [16], and the variable-stiffness transmission (VST) concept [17]. For these conceptual schemes, we investigate and compare limits of performance under safety-enforcing constraints. Based on this analysis, the variable-stiffness actuation (VSA) is considered in more detail as a candidate technology for high-performance, intrinsically safe mechanism design. Different possible technologies to implement VSA are reviewed, and control schemes for exploiting the potential of VSA are considered.

## Limits of Performance Under Safety Constraints

To lay down a principled discussion of different joint actuation schemes in terms of safety and performance, it is important to establish quantitative definitions of both these concepts. We will give definitions that attempt at not being too restrictive, although, of course, full generality cannot be hoped for with any formula for such faceted concepts.

## *Robots designed to share an environment with humans in domestic, entertainment, assistive, rehabilitation, or medical applications must fulfill different requirements from those in industry.*

### Safety

As already stated, we will only focus on a particular aspect of safety of robot manipulators, which is against unexpected collisions by the manipulator with a human operator. In the worst case, impacts could happen anywhere on the manipulator structure and on the body of the operator, and at any time during the execution of a planned trajectory. The severity of injuries caused by collisions is a well studied subject in biomechanics, with particular regard to such domains as car accidents [18], [19] or sports [20], though only very recently these studies have been applied to robotics [16]. Researchers have developed several standard indices of injury severity, including the Gadd Severity Index (GSI), the Head Injury Criterion (HIC) [19], the “3 ms” criterion, the Viscous Injury Response (VC), or the Thoracic Trauma Index (TTI). Most of these are related to a basic tolerance limit curve developed at Wayne State University (the WSUTL) on the basis of data experimentally acquired from animal and cadaver head collision tests. The WSUTL is a curve plotting head accelerations versus impact duration, indicating that very intense head acceleration is tolerable if it is very brief but that much less is tolerable if the pulse duration exceeds 10 or 15 ms (as the time exposure to cranial pressure pulses increases, the tolerable intensity decreases).

Gadd [18] plotted the WSUTL curve in log-log coordinates, obtaining a straight line of slope  $-2.5$ , and proposed accordingly a severity index as:

$$\text{GSI} = \int_0^t a^{2.5} d\tau,$$

where  $a$  is the head acceleration in grams, and the integral is extended to the whole duration of collision. A GSI value of 1,000 is generally considered to be the threshold level or tolerance limit for serious head injury.

Versace [19] proposed a mathematical refinement of the GSI known as the Head Injury Criterion (HIC), which is defined as:

$$\text{HIC} = T \left[ \frac{1}{T} \int_0^T a(\tau) d\tau \right]^{2.5},$$

where  $T$  is conventionally the final time of impact. As the choice of this time is often difficult, it is recommended to consider the worst-case HIC at varying  $T$ , which corresponds

to taking  $T$  equal to the time at which the head reaches its maximum velocity  $v(T)$  (typically,  $T \leq 15$  ms). An HIC value of 1,000 or greater is typically associated with extremely severe head injury; a value of 100 can be considered suitable to normal operation of a machine physically interacting with humans. A generalization of the HIC to collisions with other parts of the body can be considered whereby the 2.5 coefficient is replaced by other empirically determined values  $\alpha$  (see, for example, [21]) and, assuming the operator is standing still before the impact, one can write:

$$\text{HIC}' = T^{1-\alpha} v(T)^\alpha.$$

In general, evaluation of the above severity indices is numeric, based on either experimental or simulated data. However, it is instructive to compute the most widely used index, the HIC, for the basic case of a single rigid joint moving at uniform velocity  $v$  before impact, as depicted in Figure 1. In this case, by integration of the equations of motion and simple calculations, one gets

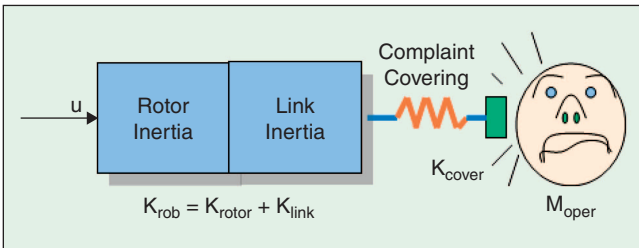


**Figure 1.** Simplified model of the impact between a rigid 1-DOF robot arm and an operator.

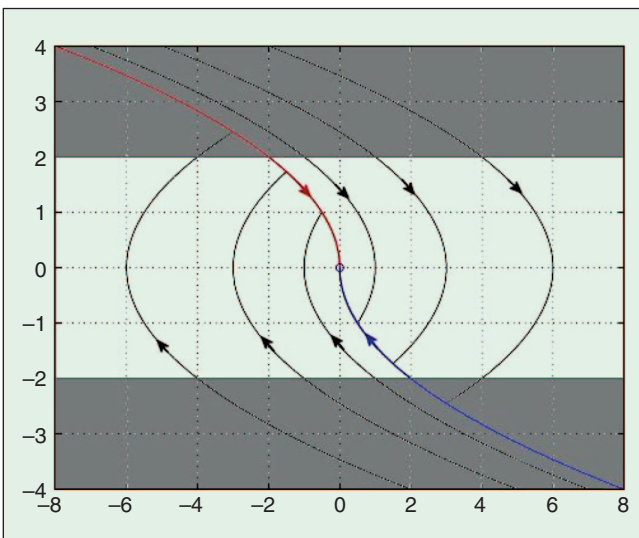


**Figure 2.** Optimal trajectories in state-space (position versus velocity) for the safe brachistochrone problem of a simple link model. The link accelerates in the first “bang” piece with  $u = \pm U_{max}$ , following a parabolic trajectory until the velocity bound  $\dot{x}_{rob} = \pm v_{safe}$  is reached; hence, velocity is held constant until the parabolic arc corresponding to  $u = \mp U_{max}$  and going to the origin of the state-space is reached.

$$\begin{aligned} \text{HIC} &= 2 \left( \frac{2}{\pi} \right)^{\frac{3}{2}} \left( \frac{K_{cov}}{M_{oper}} \right)^{\frac{3}{4}} \left( \frac{M_{rob}}{M_{rob} + M_{oper}} \right)^{\frac{7}{4}} v^{\frac{5}{2}} \\ &\stackrel{\text{def}}{=} \beta(M_{rob}, M_{oper}, K_{cov}) v^{\frac{5}{2}}, \end{aligned} \quad (1)$$

where total effective mass  $M_{rob} = M_{rotor} + M_{link}$  accounts for both the reflected rotor inertia and link inertia at the impacting section, the impacted operator mass is  $M_{oper}$ , and  $K_{cov}$  is the lumped stiffness of a compliant cover on the arm. Notice that  $\beta(\cdot) > 0$  is a function only of mechanical (inertial and compliance) parameters; hence, imposing a maximum acceptable level of injury risk at  $\text{HIC}_{max}$  implies an upper bound on the link velocity:

$$v_{safe} = \left( \frac{\text{HIC}_{max}}{\beta(\cdot)} \right)^{\frac{2}{5}}. \quad (2)$$

Using data of the second link of a lightweight arm in our lab ( $M_{rot} = 1.2$  kg,  $M_{link} = 0.1$  kg, soft rubber cover compliance  $K_{cov} = 5$  kN/m, and  $M_{oper} = 4$  kg), we have that an acceptable HIC of 100 would imply a velocity upper limit  $v_{safe} \simeq 2$  m/s.

## Performance

The second crucial step is to quantitatively define performance, or rather a *performance metric*, so that we can make informed design and control decisions.

Among many aspects of performance associated with servo-controlled mechanisms, such as robot arms, a primary concern is promptness of response, as it is, for example, classically measured in the response to a step input. Clearly, answers to such questions as “How long does it take to bring the arm from rest to rest at a prescribed position?” depend on two factors: the mechanical design and the adopted control law. Indeed, ideal control laws with endless actuator authority could be perfectly fast, while remaining perfectly safe. Even in the real world of real (hence, limited-torque) actuators, the infinite variety of different controllers would produce different performance and cause different risks for the same mechanical design.

It is, therefore, important that we decouple the mechanical and the control design problems. This can be done if an “absolute enough” performance measure is adopted, which abstracts away the possible controller choices in this phase, allowing one to concentrate on the intrinsic properties of the mechanism. In other words, we should like to use the *best possible controller* with all different mechanisms we are interested in examining, and compare their performance in such ideal conditions.

A measure of how fast a given mechanism can be brought to a desired configuration, under limited actuator authority and with safety guarantees, but with an ideally smart control, is its *safe brachistochrone*, that is the solution to the following problem:

For a mechanism with total inertia and actuator limits given, find the minimum time necessary to move

between two fixed configurations such that at any instant during the motion an unexpected impact with the device would produce a injury severity index below safety levels.

Such problem formulation lends itself to a direct interpretation in terms of a minimum time optimal control problem. For instance, the safe brachistochrone for the basic case of Figure 1, with bounded actuator torque  $u \leq U_{\max}$ , can be written mathematically as

$$\begin{cases} \min_T \int_0^T 1 dt \\ M_{\text{rob}} \ddot{x}_{\text{rob}} = u \\ |\dot{x}_{\text{rob}}| \leq v_{\text{safe}} \\ |u| \leq U_{\max} \end{cases} \quad (3)$$

with initial and terminal conditions

$$\begin{cases} x_{\text{rob}}(0) = 1, \dot{x}_{\text{rob}}(0) = 0, \\ x_{\text{rob}}(T) = 0, \dot{x}_{\text{rob}}(T) = 0. \end{cases}$$

In this case, an explicit solution for the optimal control can be obtained analytically by application of Pontryagin's Maximum Principle [22]. It can be easily shown [23] that optimal trajectories in this case are of the “bang-zero-bang” type and consist, in general, of three extremal arcs corresponding to either saturated torque ( $u = \pm U_{\max}$ ) or unforced motion ( $u = 0$ ) (see Figure 2). Correspondingly, the minimum time  $T_{\text{opt}}$  for any given initial condition is a monotonically decreasing function of  $U_{\max}$  and  $v_{\max}$ . In particular, the relationship between performance (minimum time to reach the origin) and the acceptable level of injury risk reported in Figure 3 shows how performance is inevitably degraded by imposing increasingly high safety constraints. It is important to note that to recover minimum-time performance, only mechanical design changes can be effective, as the control resources are exhausted by optimal control. Assuming that total link inertia is minimized, and that covering compliance cannot be further increased, a possibility for performance enhancement is left with the design of nonrigid mechanical transmission.

### Passive Elastic Transmission

While several different approaches have been proposed for the mechanical design of inherently safe arms, the vast majority use elastic joints (Figure 4). The basic idea behind the purposeful introduction of compliance in the joint transmission is that of decoupling the inertia of the actuator proper (which is very relevant, especially for geared actuators) from the inertia of the link. The achieved decoupling is dynamic, and acts stronger at high frequencies, thus smoothing out the impact force curve and reducing potential danger. The positive effect of transmission elasticity on safety is illustrated in Figure 5, where the HIC (computed by simulations) of the impact between an elastically actuated link moving at uniform velocity and an operator is reported at varying

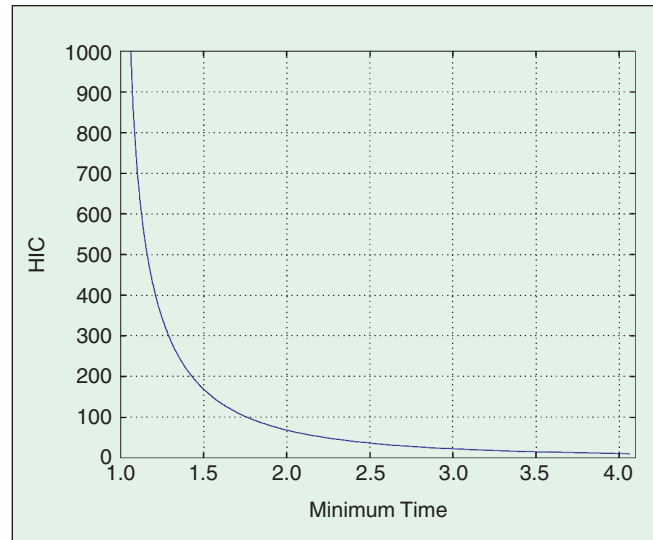


Figure 3. The safety-performance tradeoff curve for the rigid single joint case.

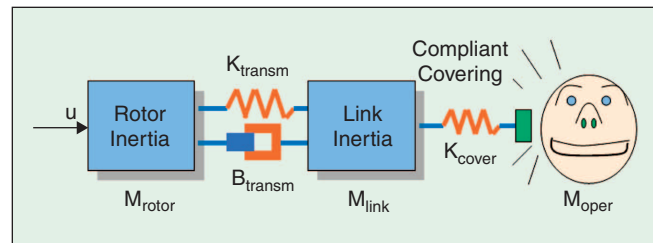


Figure 4. The interposition of an elastic transmission between the actuator and the link is a classical approach for reducing injury risks.

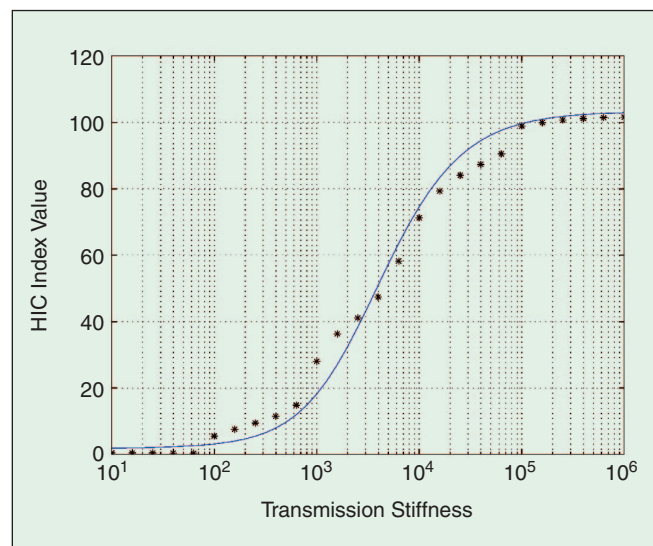


Figure 5. Head-injury coefficients evaluated for the impact of a link of effective inertia  $M_{\text{link}} = 0.1$  kg elastically coupled to a rotor of inertia  $M_{\text{rot}} = 1.2$  kg by a transmission with  $B_{\text{transm}} = 0$ , as  $K_{\text{transm}}$  varies. The rotor and link are assumed to move uniformly at velocity  $v = 10$  m/s before impact. Data points are obtained by simulation, while the solid curve is calculated using the compound inertia formula (4).

the transmission stiffness  $K_{\text{transm}}$ . Note explicitly that, in the limit  $K_{\text{transm}} \rightarrow \infty$ , the HIC tends to the value obtained by (1) in the rigid link case, while, for  $K_{\text{transm}} \rightarrow 0$ , only the link inertia  $M_{\text{link}}$  is relevant to HIC.

HIC data in Figure 5 are obtained via accurate numeric integration of the equations of motion after impact. An approximate evaluation of the HIC for different values of the transmission compliance can be obtained via (1), introducing a compound inertia  $M_{\text{rob}}$  to take into account the elastic coupling between  $M_{\text{rot}}$  and  $M_{\text{link}}$  as:

$$M_{\text{rob}}(K_{\text{transm}}) = M_{\text{link}} + \frac{K_{\text{transm}}}{K_{\text{transm}} + \gamma} M_{\text{rot}}. \quad (4)$$

The compound inertia of the elastic joint is then a function of  $K_{\text{transm}}$  linearly interpolating the two limit cases of perfect decoupling and rigid joint. By choosing  $\gamma = 3,000$  in our example, (4) and (1) provide the HIC curve shown in (5), well fitting simulation data while substantially reducing calculations.

The downside of elastic coupling is clearly performance degradation. Intuitively, compliant transmission tends to respond slowly to torque inputs on the actuator and to oscillate around the goal position, so that it can be expected that the promptness of an elastically actuated arm is severely reduced if compliance is high enough to be effective on safety

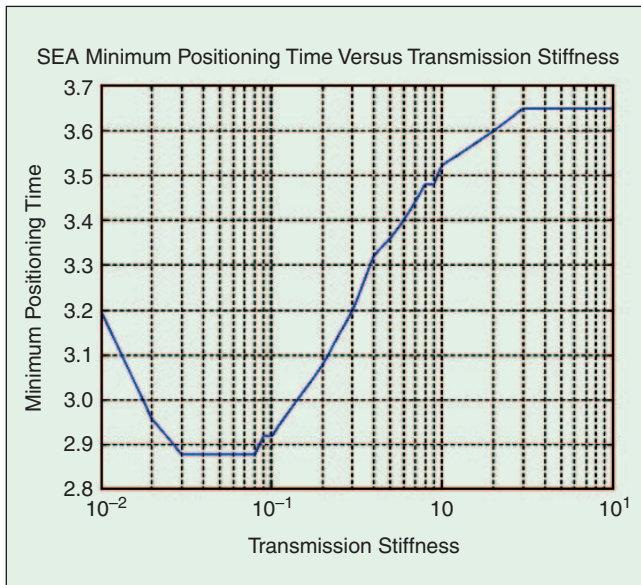


**Figure 6.** The minimum time necessary to reach a given positional goal under safety constraints and actuator saturation, as a function of the transmission stiffness, for an elastic transmission.

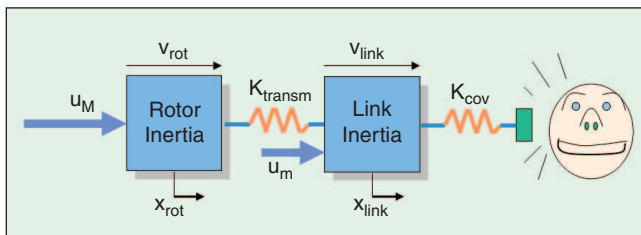


**Figure 7.** A conceptual illustration of the  $DM^2$  approach.

accounts. The problem of controlling passively elastic joints so as to recover performance has been studied at length in the robotics literature, both in the general case [24]–[28] and the review in [29] and in safety-oriented design contexts [30], [31]. Because, in general, the response would depend on the specific control algorithm applied, it is interesting to our purposes to apply our control-optimal performance metric to evaluate the most prompt response possible. The safe brachistochrone problem can be posed in this case as:

$$\begin{cases} \min_T \int_0^T 1 dt \\ M_{\text{rot}} \ddot{x}_{\text{rot}} + K_{\text{transm}}(x_{\text{rot}} - x_{\text{link}}) = u \\ M_{\text{link}} \ddot{x}_{\text{link}} + K_{\text{transm}}(x_{\text{link}} - x_{\text{rot}}) = 0 \\ |\dot{x}_{\text{link}}| \leq v_{\text{safe}}(K_{\text{transm}}) \\ |u| \leq U_{\text{max}}, \end{cases}$$

with initial and terminal conditions:

$$\begin{cases} x_{\text{rot}}(0) = 1, \dot{x}_{\text{rot}}(0) = 0 \\ x_{\text{link}}(0) = 1, \dot{x}_{\text{link}}(0) = 0 \\ x_{\text{rot}}(T) = 0, \dot{x}_{\text{rot}}(T) = 0 \\ x_{\text{link}}(T) = 0, \dot{x}_{\text{link}}(T) = 0, \end{cases}$$

Here, the safety constraint has been imposed by limiting the impacting link velocity such that the admissible level of injury risk is never trespassed in the execution of motion. In particular, the value of  $v_{\text{safe}}$  is now a function of the transmission stiffness, which is calculated by using the compound inertia formula (4) in (2). With this assumption, the safe brachistochrone for an elastic joint can be found by numerical methods such as those described in [23]. Results reported in Figure 6 show how the shortest time to reach a given goal is a function of the joint elasticity. The performance, considered as the inverse of such minimum time, is low for high stiffness, as the high reflected inertia forces, in this case, very low maximum velocities. On the other hand, too low a transmission stiffness is not beneficial to performance either, because of the limited mechanical bandwidth. The diagram in Figure 6 indicates an optimum value of transmission stiffness (for the given inertial parameters), whereby the best performance within safety bounds is achieved.

## Recovering Performance

As already argued, although several techniques have been devised to efficiently control elastic-joint arms, the intrinsic performance limitation illustrated by the safe brachistochrone can only be overcome by modifying the mechanical design and introducing a somewhat more complicated actuation mechanism. Two such concepts have been recently proposed in this context: the  $DM^2$  approach and the VST approach.

### $DM^2$ Actuation

The  $DM^2$  approach [16] mainly consists in dividing torque generation among two actuators, of which one is devoted to low-frequency components of the required torque supply, while the other is designed for the high-frequency part. The

two motors are connected in parallel to the same joint: the slow one, which provides high torque at the cost of large rotor inertia, is coupled through a passive elastic transmission; the fast motor, with limited torque but very low rotor inertia, is rigidly connected to the joint. A conceptual model of the DM<sup>2</sup> is shown in Figure 7. If compared with the scheme of Figure 4, one notes that the torque source  $u$  is now split in two separate actuators ( $u_M$  and  $u_m$ ), for which the joint elasticity  $K_{\text{transm}}$  acts as a compliant coupling. The safe brachistochrone problem for the DM<sup>2</sup> scheme can be written as:

$$\begin{cases} \min_T \int_0^T 1 dt \\ M_{\text{rot}} \ddot{x}_{\text{rot}} + K_{\text{transm}}(x_{\text{rot}} - x_{\text{link}}) = u_M \\ M_{\text{link}} \ddot{x}_{\text{link}} + K_{\text{transm}}(x_{\text{link}} - x_{\text{rot}}) = u_m \\ |\dot{x}_{\text{link}}| \leq v_{\text{safe}}(K_{\text{transm}}) \\ |u_M| \leq U_{M,\text{max}} \\ |u_m| \leq U_{m,\text{max}} \end{cases}$$

with initial and terminal conditions:

$$\begin{cases} x_{\text{rot}}(0) = 1, \dot{x}_{\text{rot}}(0) = 0 \\ x_{\text{link}}(0) = 1, \dot{x}_{\text{link}}(0) = 0 \\ x_{\text{rot}}(T) = 0, \dot{x}_{\text{rot}}(T) = 0 \\ x_{\text{link}}(T) = 0, \dot{x}_{\text{link}}(T) = 0. \end{cases}$$

For comparison, we will assume that the overall available torque is unchanged, i.e.,  $U_{M,\text{max}} + U_{m,\text{max}} = U_{\text{max}}$ . Notice that  $M_{\text{rot}}$  indicates the rotor inertia of the high-torque actuator, while  $M_{\text{link}}$  is thought to include the light-weight rotor inertia. The limit value  $v_{\text{safe}}$  is approximated as before. The safe brachistochrone for the DM<sup>2</sup> actuation scheme for different values of the coupling stiffness, computed numerically [23], is reported in Figure 8. Results in Figure 8 com-

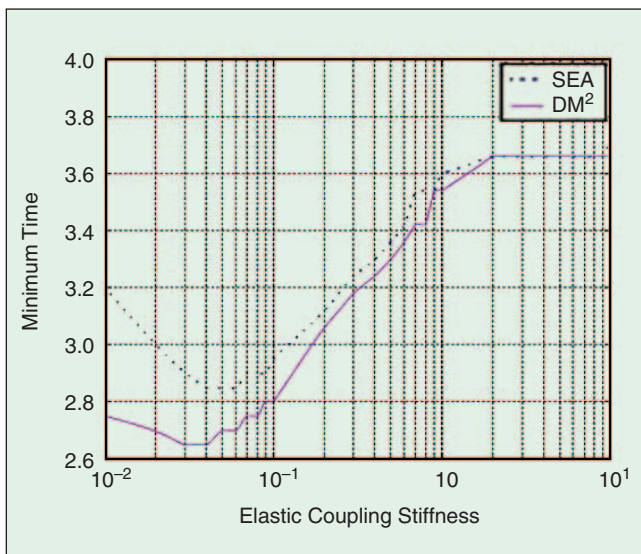


**Figure 8.** Minimum time to goal under safety constraints and actuator saturation as a function of the elastic coupling stiffness, for a DM<sup>2</sup> actuation scheme. Results previously obtained for a passive elastic transmission are shown (dashed) for reference.

## The inherent danger to humans of conventional arms can be mitigated by drastically increasing their sensorization and/or by modifying their controllers.

pare favorably with those obtained in Figure 6 for passively elastic transmission and demonstrate the feasibility of an appreciable performance recovery. This is true in particular for rather large transmission compliance, while there is almost no difference in performance for stiff coupling (as it was to be expected).

### Variable Stiffness Transmission

A second approach to gain in performance for guaranteed-safety joint actuation schemes consists in allowing the passive compliance of transmission to vary during the execution of tasks. Figure 9 is a conceptual drawing illustrating such a VST scheme. While we defer discussion of how such variation of transmission stiffness can be obtained in practice to a later section, we should like to discuss here the expected advantages of the scheme. Consider, for example, a classical velocity profile for the actuation of a rest-to-rest motion of a joint (the top of Figure 10), consisting of an initial ramp accelerating from zero

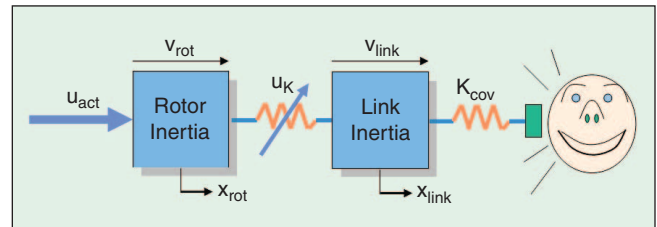


**Figure 9.** The concept of VST consists of allowing the elasticity of the transmission  $K_{\text{transm}}$  to be a controlled variable during execution of a task.

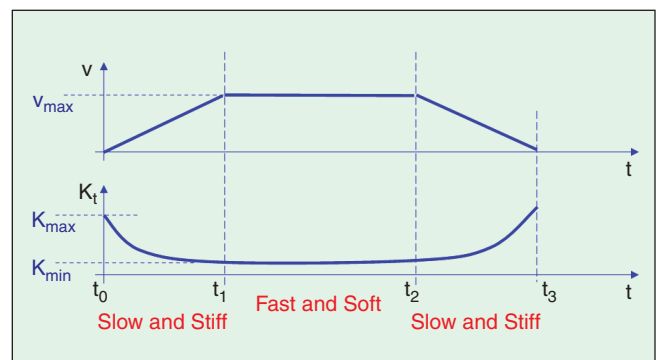


**Figure 10.** The intuitive behavior of a VST in a 1-DOF rest-to-rest task. High stiffness is imposed at low velocities, while transmission compliance is introduced at high velocities to reduce potential impact injuries.

to maximum velocity, a uniform velocity part, and a final descending ramp decelerating again to zero. At a rather intuitive level, it would be desirable that the joint have low stiffness in the high velocity phase, so as to minimize reflected inertia and thus injury risks. On the other hand, it would seem appropriate to have as high a stiffness as possible in the early accelerating phase so as to allow the actuator to put the link in motion swiftly, and in the final deceleration, where oscillations have to be minimized. To verify possible advantages of the VST scheme, let us consider again the safe brachistochrone problem, assuming now that the transmission stiffness is a control variable  $u_K$  subject to lower and upper limits:

$$\begin{cases} \min_T \int_0^T 1 dt \\ M_{\text{rot}} \ddot{x}_{\text{rot}} + u_K (x_{\text{rot}} - x_{\text{link}}) = u_{\text{act}} \\ M_{\text{link}} \ddot{x}_{\text{link}} + u_K (x_{\text{link}} - x_{\text{rot}}) = 0 \\ |\dot{x}_{\text{link}}| \leq v_{\text{safe}}(u_K) |u_{\text{act}}| \leq U_{\text{max}} \\ u_{K,\min} \leq u_K \leq u_{K,\max} \end{cases}$$

with initial and terminal conditions:

$$\begin{cases} x_{\text{rot}}(0) = 1, \dot{x}_{\text{rot}}(0) = 0 \\ x_{\text{link}}(0) = 1, \dot{x}_{\text{link}}(0) = 0 \\ x_{\text{rot}}(T) = 0, \dot{x}_{\text{rot}}(T) = 0 \\ x_{\text{link}}(T) = 0, \dot{x}_{\text{link}}(T) = 0. \end{cases}$$

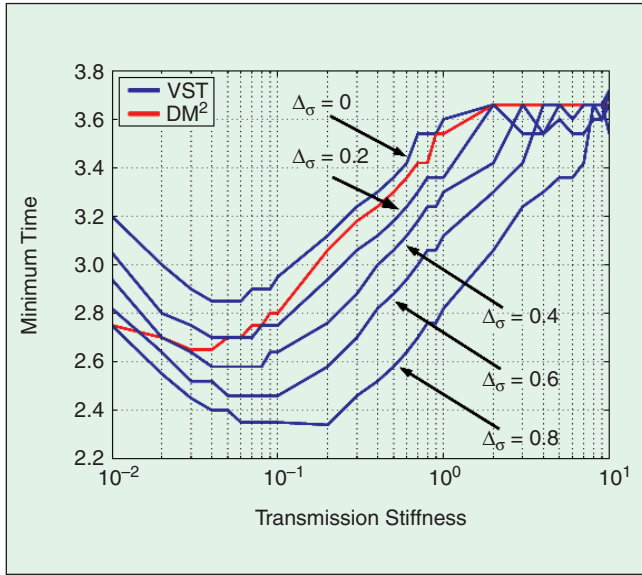


**Figure 11.** Minimum time to goal under safety constraints and actuator saturation for a VST scheme, as a function of the stiffness center value  $\bar{\sigma}$  and for different stiffness ranges  $\Delta\sigma$ . Previously obtained results are reported for reference.

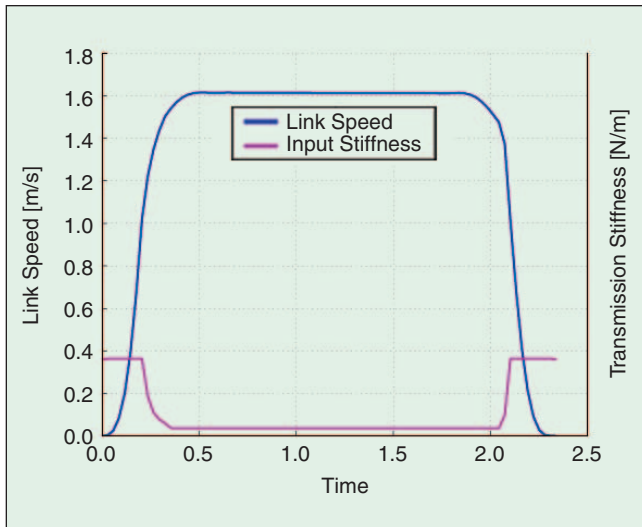


**Figure 12.** Optimal joint stiffness and velocity during a rest-to-rest task.

The optimal control problem, somewhat more involved here than in previous cases due to the nonlinearity of the dynamics, was solved numerically [23], and results are reported in Figure 11. As it can be expected, the effectiveness of VST depends on the affordable range of compliance at the joint, the best performance being obtained in the limit case that the transmission could be controlled to be either perfectly compliant or stiff ( $u_{K,\min} = 0$ ,  $u_{K,\max} = \infty$ ) (see Figure 11). Considering a symmetric range of controllable stiffness:

$$u_{K,\min} = (1 - \Delta\sigma)\bar{\sigma} \quad u_{K,\max} = (1 + \Delta\sigma)\bar{\sigma},$$

one can observe from Figure 11 that performance can be improved beyond that of  $DM^2$  for  $\Delta\sigma \geq 0.5$ . It is also noteworthy that, for  $\Delta\sigma = 0$ , the same results of Figure 6 are obtained again (modulo slight numerical differences). Figure 12 shows the diagrams of joint velocity  $\dot{x}_{\text{link}}$  and compliance  $u_K$  obtained along the optimal solution of the safe brachistochrone of a VST joint with  $\bar{\sigma} = 0.2$  and  $\Delta\sigma = 0.8$ . The diagrams confirm that an effective VST control policy should suitably blend slow-and-stiff and fast-and-soft phases, as anticipated in Figure 10 (notice stiffness saturation in the initial and final phases). It is fair to point out that the very positive results by the VST scheme would probably be somewhat lowered, should a realistic mechanism for implementing variable stiffness be considered, by, for example, making stiffness adaptation slower. However, we believe that the analysis above still provides an useful insight in the relative merits and shortcomings of the two actuations schemes and might even suggest alternative solutions.

### Implementation of the VST Concept

While we have shown that the concept of VST can be an effective means of dealing with the safety/performance trade-off, in this section we will briefly review some possible implementations of the mechanics and control of VST systems and discuss their relative advantages and disadvantages, so as to provide some background and directions to explore in the realization of intrinsically safe, efficient actuation mechanisms.

#### Mechanical Implementation

The implementation of safe actuation mechanisms based on passive transmission elasticity and on  $DM^2$  has been consid-

ered in detail in [30] and [16], respectively. As to VST, a first, direct approach is to implement a mechanism that can mechanically vary its compliance by means of adjustable-length leaf springs, for example. The idea has been introduced very early in robotic assembly to achieve passive impedance [32], [33] and has attracted renewed attention more recently for the design of humanoids and human-friendly robots [34], [31]. The possibility of introducing a controllable amount of damping in the transmission using magnetic brakes [34] or electro- or magneto-rheological fluids [35] has been also envisioned. Mechanical impedance adjusters typically require two actuators per independently controlled joint (one for the joint motion and one for the adjuster), and tend to be rather bulky in their implementation if the adjuster actuator is placed at the joint. In [31], a clever design of a three-degree-of-freedom (3-DOF) anthropomorphic shoulder mechanism with programmable passive compliance was described with reduced encumbrance and number of actuators (at the cost of coupling the compliance of different DOFs).

A second approach that has been followed in the design of tunable passive compliance joints is the *antagonistic* concept. The approach takes its name by analogy to the organization of biological muscular apparatuses (see [36], for example). To build an antagonistic VST, different technologies can be adopted, ranging from very simple to sophisticated. Indeed, some commercial actuators, such as low-friction two-way air cylinders (see Figure 13), are already intrinsically suited to this function.

A rotary VST joint is illustrated in Figure 14. Here, two actuators (for instance, conventional electric motors) are connected to the same joint in an antagonistic arrangement through mechanically compliant elements (depicted as springs). Notice that the two actuators need only be operable one-way (e.g., pull-only). It is interesting to derive a simple model of this mechanism. The torque  $\tau$  applied to the joint, corresponding to a joint angle  $q$ , actuator angular positions  $\theta_1$  and  $\theta_2$ , is given by:

$$\tau = R(k_1 L_1 - k_2 L_2), \quad (5)$$

with  $k_1, k_2$  the spring stiffness coefficients,  $L_1 = r\theta_1 - Rq$  and  $L_2 = r\theta_2 + Rq$  their elongations,  $R$  the radius of the joint pulley, and  $r$  the radius of the actuator pulleys.

The effective joint stiffness  $\sigma$ , defined as the infinitesimal variation of the joint torque corresponding to an infinitesimal change of joint angle, while inputs to actuator are held constant (no reliance is thus made on feedback control of actuators in case of impacts), is simply evaluated as:

$$\sigma = \frac{\partial \tau}{\partial q} = R^2(k_1 + k_2) - R^2 \left( \frac{\partial k_1}{\partial L_1} L_1 + \frac{\partial k_2}{\partial L_2} L_2 \right). \quad (6)$$

It can be easily observed that, if stiffness coefficients  $k_i$  are constant, the overall joint stiffness is independent of the actuator inputs. To realize a VST with this scheme, nonlinear elastic elements with coefficient  $k_i(L_i)$ , depending on the

elongation, are therefore in order. In the common case that the two springs are equal and have bounded elongation  $L_{\min} \leq L_i \leq L_{\max}$ ,  $i = 1, 2$ , we have that the stiffness range (which was shown in the previous section to directly affect performance) evaluates to

$$\Delta\sigma = \frac{\sigma_{\max} - \sigma_{\min}}{\sigma_{\max} + \sigma_{\min}} = \frac{L_{\max} - L_{\min}}{\bar{\sigma}} \frac{\partial k}{\partial L}.$$

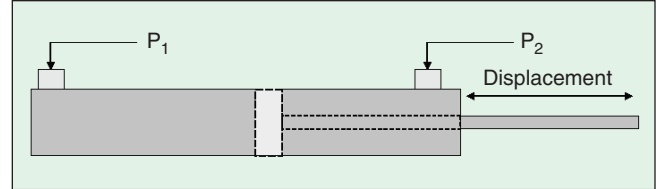


**Figure 13.** Even a simple off-the-shelf two-way air cylinder can be used as a linear VST actuator. Increasing air pressure in proportion in both chambers increases the overall stiffness of the rod, while the equilibrium of the rod under an external load can be displaced by a differential in chamber pressure.

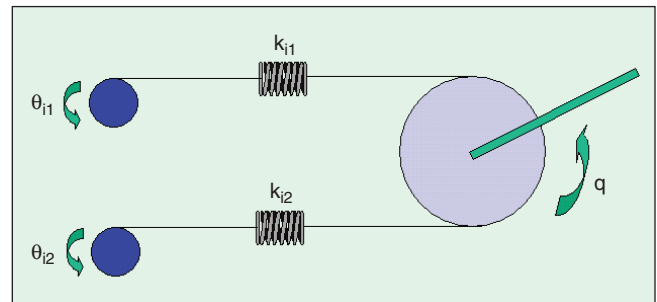


**Figure 14.** An antagonistic arrangement of two actuators on a joint to control joint position and stiffness independently.

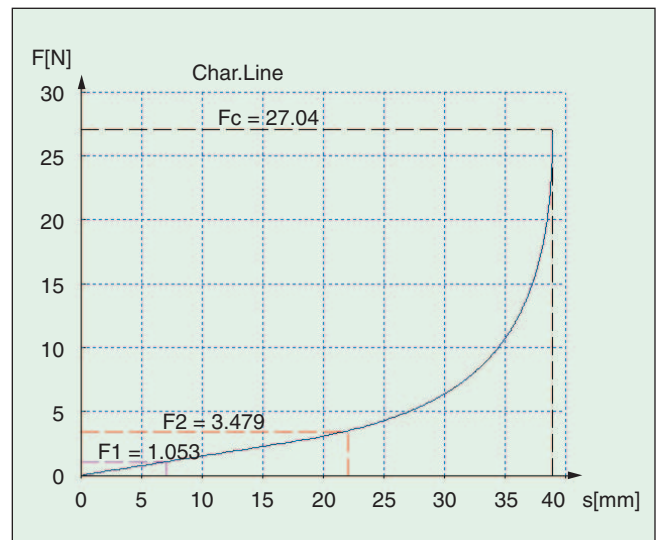


**Figure 15.** The force-length characteristic curve of a helical conical spring, obtained by the Hexagon Spring Software [37]. In the length range  $L_{\min} = 22$  mm,  $L_{\max} = 38$  mm, the force curve is approximately parabolic with  $k(L) = 1.47L - 28.8$ .

**Another approach to increasing the safety level of robot arms interacting with humans is to intentionally introduce mechanical compliance in the design.**

To implement nonlinear elastic elements, different arrangements can be conceived, among which helical conical springs are perhaps the most common example. Nonlinearity of the force/length curve (see Figure 15) depends on the flattening of outer coils, when the conical spring is used in compression. By careful design and suitable preloading, conical springs can be made to work in the nonlinear region, where the force

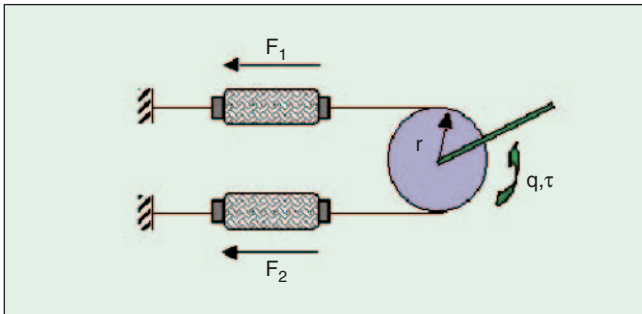


**Figure 16.** Model of a VST joint actuated by two antagonistic McKibben actuators.

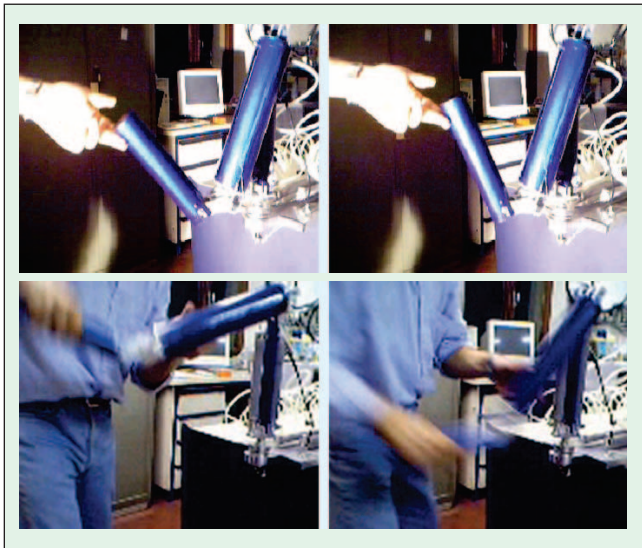


**Figure 17.** The University of Pisa SoftArm has a 3-DOF anthropomorphic and lightweight structure, actuated by McKibben artificial muscles in antagonistic pairs. The arm can interact closely with a human operator in both low- (top) and high-frequency (bottom) ranges.

curve is approximately parabolic. An advantage of employing two identical springs with parabolic force/length characteristic in the antagonistic scheme is that the resulting joint stiffness is independent from the joint angle ( $\partial\sigma/\partial q = 0$ ). However, helical conical springs tend to be rather cumbersome if a large enough range of joint stiffness is required to meet performance specs. For instance, from the data reported in Figure 15, a spring designed to work in the range  $L_{\min} = 22$  mm,  $L_{\max} = 38$  mm achieves only  $\Delta\sigma = 0.2$ .

An interesting alternative to implement tunable passive compliance is provided by McKibben artificial muscles [38]–[41] (Figure 16). These are pneumatic actuators consisting of an inner inflatable tube, closed at the ends and surrounded by braided cords. A simple, yet accurate, model for a McKibben muscle proposed by [39] is summarized as

$$f = k(L^2 - L_{\min}^2)p,$$

where  $f$  is the applied force,  $p$  is the pressure in the inner tube,  $L$  is the actuator elongation,  $k$  and  $L_{\min}$  are constant parameters depending on constructive details. The model is valid in the operating region  $L_{\min} \leq L \leq L_{\max}$ , where  $f > 0$ . For a robot joint actuated by two identical McKibben actuators in antagonistic arrangement, as shown in Figure 16, the joint characteristic functions for joint torque  $\tau$  and stiffness  $\sigma = \partial\tau/\partial q$ , assuming commands to be control pressures,  $p = (p_1 \ p_2)^T$ , are obtained as:

$$\begin{bmatrix} \tau \\ \sigma \end{bmatrix} = \begin{bmatrix} Rk(L_1^2 - L_{\min}^2) & Rk(L_2^2 - L_{\min}^2) \\ -2R^2kL_1 & -2R^2kL_2 \end{bmatrix} p. \quad (7)$$

Evaluating the stiffness range for this arrangement, at equilibrium in the  $q = 0$  configuration (where  $L_1 = L_2 = (L_{\min} + L_{\max})/2 = \bar{L}$  and  $p_1 = p_2$ ), one has:

$$\Delta\sigma = \frac{p_{\max} - p_{\min}}{p_{\max} + p_{\min}}.$$

Using a moderate pressure range ( $p_{\min} = 0.5$  bar,  $p_{\max} = 4.5$  bar), a significant stiffness variation of  $\Delta\sigma = 0.8$  is obtained.

The linear map (7) is invertible within the operating region of the two actuators, hence, one can quite straightforwardly compute the inputs to obtain a desired joint torque and compliance as:

$$p = \begin{bmatrix} -\frac{1}{d}2R^2kL_2 \\ \frac{1}{d}2R^2kL_1 \end{bmatrix} \tau + \begin{bmatrix} \frac{1}{d}Rk(L_2^2 - L_{\min}^2) \\ \frac{1}{d}Rk(L_1^2 - L_{\min}^2) \end{bmatrix} \sigma. \quad (8)$$

The space of actuator commands can thus be regarded as the Cartesian product of the two subspaces of noninteracting torque-generating commands and contraction stiffening commands.

Based on these considerations, McKibben artificial muscles can probably be considered among the best candidates within readily available actuators to implement the VST scheme. We adopted antagonistic McKibben actuators in the implementation of an experimental 3-DOF VST arm described in [17] (see Figure 17). However, McKibben actuators do have several disadvantages, such as rather slow response, parasitic conduit capacitance, and the necessity of a pressurized main air source (which renders them unsuitable to applications such as humanoid robots). A possible alternative in the short term could be provided by innovative electromechanical design focusing specifically on implementation of the VST concept, and, in a longer time-scale, by emerging technologies such as polymeric gels, nanotubes, or electroactive polymers [42], [43].

### Control Implementation

The problem of controlling arms with passive, constant compliance has been studied extensively in the robotics literature (see [44] and [24] for examples), albeit often without a direct relation to safety of operations. Techniques for accurately controlling positions exist, which are based on advanced nonlinear control techniques (see [25], for example) and typically assume knowledge of accurate models of inertial and compliance parameters. Adaptive control methods that could cope with uncertain inertia in elastic joints have also been studied (as cited in [45]), although adapting to unknown stiffness parameters appears to be a tougher problem, due to the fact that compliance parameters enter nonlinearly in the dynamic equations.

For robot arms with VST, the control problem is clearly more faceted as it also involves the continuous change of joint stiffness and is virtually an untouched subject so far (up to our knowledge). We confine ourselves to describe the problem in its generalities here and to describe some possible solutions and research directions.

Naturally, the dynamic control of tunable compliant arms inherits many of the problems with the control of flexible arms, but they can only partially enjoy solutions provided in that field. A key difference is the presence of essential nonlinearities in the model of soft arms, which obviously make control much harder. This is particularly true when an exact model of the system parameters is not available, and adaptation is necessary.

An important control objective is to guarantee that arbitrary trajectories of the end-effector can be controlled while stiffness is controlled to desired values, without the two specifications interfering with each other (decoupled control). Some results in this direction have been presented in [17].

A first necessary element of a VST control systems would be a planning algorithm to provide reference motion and stiffness trajectories. The planner should take into account the insight gained by solving the safe brachistochrone problem for a VST joint by blending slow-and-stiff and fast-and-soft phases, so as to guarantee safety (with adequate margins) of the nominal motion. Execution of such nominal motion despite disturbances and modeling inaccuracies should then be

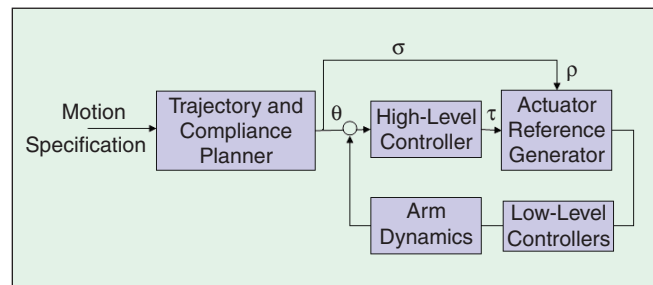


**Figure 18.** A conceptual description of a control system for VST arms.

enforced by a closed-loop control scheme. A possible organization of the control system for a VST arm, depicted in Figure 18, is described as follows:

- 1) For given motion specifications (e.g., rest-to-rest motions of the arm joints with required safety level), the trajectory and compliance planner (TCP) block computes offline the optimal reference profile for joint positions  $\theta$  and stiffness  $\sigma$  (as cited in Figure 12). The role of the TCP is similar to that of a Cartesian-to-joint reference translator in conventional arm controllers.
- 2) The HLC computes joint torques  $\tau$  as a function of joint-position tracking errors, just like a standard joint controller implementing a proportional integral derivative (PID), for example, or computed torque scheme.
- 3) Based on such a torque request and on the stiffness reference, the actuator reference generator (ARG) block computes set values for the individual motors actuating the VST arm. For instance, an ARG for an antagonistic McKibben arrangement, as in Figure 16, would simply implement the inverse map (8), computing set muscle values  $p$ .
- 4) Low-level controllers (L.L.C.) would only take care of closing a fast inner loop to ensure that actuators actually follow their set values (typically, commercial actuator drivers implement this block).

Alternatives to the conceptual scheme of Figure 18 can be devised by aspiring to the biomechanical theory of human motion [46], for example. For instance, the internal model theory admits the existence of a (learned) dynamic model of the human arm in its sensory-motor control. Such a model, with unknown constant parameters, is continuously adapted by a feedback adaptive control that generates the model parameters estimation [47]. A thorough theoretical and experimental study of these different approaches to control is in order to evaluate relative merits and possible convergence of the different approaches to the control of variable stiffness arms.

### Conclusion

The problem of achieving high performance with a mechanism that is safe to humans interacting directly with it poses many challenging technological problems. We have considered the problem of designing joint-actuation mechanisms that can allow fast and accurate operation of a robot arm

while guaranteeing a suitably limited level of injury risk. Different approaches to the problem have been presented, and a method of performance evaluation has been proposed based on minimum-time optimal control with safety constraints. In our opinion, VST is one of a few different possible schemes that allows the most flexibility and potential performance. Some aspects related to the implementation of the mechanics and control of VST actuation were also reported.

## Acknowledgments

The useful work of undergraduate students Michele Bavaro and Marco Piccigallo is gladly acknowledged. This work was partially supported by EC contracts IST-2001-38040 (TOUCH-HAPSYS under FET Presence Initiative) and IST-2001-37170 (RECSYS).

## Keywords

Soft robotics, safety, performance recovering, variable stiffness transmission.

## References

- [1] H. Kumamoto, Y. Soto, and K. Inoue, "Hazard identification and safety assessment of human-robot systems," *Eng. Risk and Hazard Assessment*, vol. 1, pp. 61–80, 1986.
- [2] K. Ikuta, H. Ishii, and M. Nokata, "Safety evaluation method of design and control for human-care robots," *Int. J. Robot. Res.*, vol. 22, no. 5, pp. 281–297, May 2003.
- [3] G. Giralt and P. Corke, Eds., *Technical Challenge for Dependable Robots in Human Environments*. Seoul, Korea: IARP/IEEE Workshop, 2001.
- [4] *ISO/IEC Guide 51: Safety Aspects—Guidelines for Their Inclusion in Standards*, 1999.
- [5] J. Adams, R. Bajcsy, J. Kosecka, V. Kumar, R. Mandelbaum, M. Mintz, R. Paul, C. Wang, Y. Yamamoto, and X. Yun, "Cooperative material handling by human and robotic agents: Module development and system synthesis," in *Proc. IEEE/RSJ Int. Conf. Intell. Robots and Syst.*, 1995, Pittsburgh, PA, pp. 200–205.
- [6] O. Khatib, K. Yokoi, O. Brock, K.-S. Chang, and A. Casal, "Robots in human environments: Basic autonomous capabilities," *Int. J. Robot. Res.*, vol. 18, pp. 684–696, 1999.
- [7] T. Noritsugu, T. Tanaka, and T. Yamanaka, "Application of rubber artificial muscle manipulator as a rehabilitation robot," in *Proc. IEEE Int. Workshop Robot and Human Communication*, Tsukuba, Japan, Nov. 11–14, 1996, pp. 112–117.
- [8] J. Guiochet and A. Vilchis, "Safety analysis of a medical robot for tele-echography," in *2d IARP IEEE/RAS Joint Workshop Tech. Challenge for Dependable Robots Human Environments*, Toulouse, France, Oct. 2002, pp. 217–227.
- [9] E. Cheung and V. Lumelsky, "Proximity sensing in robot manipulator motion planning: System and implementation issues," *IEEE Trans. Robot. Automat.*, no. 5, pp. 740–751, 1989.
- [10] H. Iwata, H. Hoshino, T. Morita, and S. Sugano, "Force detectable surface covers for humanoid robots," in *Proc. IEEE/ASME Int. Conf. Advanced Intell. Mechatronics*, Como, Italy, July 8–11, 2001, pp. 1205–1210.
- [11] K. Salisbury, W. Townsend, B. Eberman, and D. DiPietro, "Preliminary design of a whole-arm manipulation system (WAMS)," in *Proc. 1988 IEEE Int. Conf. Robot. Automat.*, Philadelphia, PA, 1988, pp. 254–260.
- [12] G. Hirzinger, A. Albu-Schäffer, M. Hähle, I. Schaefer, and N. Sporer, "On a new generation of torque controlled light-weight robots," in *IEEE Int. Conf. Robot. Automat.*, Seoul, Korea, 2001, pp. 3356–3363.
- [13] P. Kazanzides, J. Zuhars, B. Mittelstadt, and R.H. Taylor, "Force sensing and control for surgical robot," in *Proc. Int. Conf. Robot. Automat.*, Nice, France, 1992.
- [14] J. Heinzmann and A. Zelinsky, "The safe control of human-friendly robots," in *Proc. IEEE/RSJ Int. Conf. Intell. Robots and Syst.*, Kjongju, Korea, 1999, pp. 1020–1025.
- [15] A. Albu-Schäffer and G. Hirzinger, "Artesian compliant control strategies for light-weight, flexible joint robots," in *Control Problems in Robotics*, vol. 4 (*Springer Tracts in Advanced Robotics—STAR*), A. Bicchi, H.I. Christensen, and D. Prattichizzo, Eds. Berlin, Germany: Springer-Verlag, 2003.
- [16] M. Zinn, O. Khatib, B. Roth, and J.K. Salisbury, "A new actuation approach for human friendly robot design," in *Proc. Int. Symp. Experimental Robotics—ISER'02*, Sant'Angelo d'Ischia, Italy, 2002.
- [17] A. Bicchi, S. Lodi Rizzini, and G. Tonietti, "Compliant design for intrinsic safety: General issues and preliminary design," in *Proc. IEEE/RSJ Int. Conf. Intell. Robots and Syst.*, Maui, Hawaii, 2001, pp. 1864–1869.
- [18] C.W. Gadd, "Use of weighted impulse criterion for estimating injury hazard," in *Proc. 10th Stapp Car Crash Conf.*, New York, 1966, pp. 164–174.
- [19] J. Versace, "A review of the severity index," in *Proc. 15th Stapp Car Crash Conf.*, 1971, New York, pp. 771–796.
- [20] G.O. Njus, Y.K. Liu, and T.A. Nye, "The inertial and geometrical properties of helmets," *Med. Sci. Sports Exerc.*, vol. 16, no. 5, pp. 498–505, 1984.
- [21] D.W.A. Brands, "Predicting brain mechanics during closed head impact—Numerical and constitutive aspects," Ph.D. dissertation, University of Eindhoven, Eindhoven, The Netherlands, 2002.
- [22] L.S. Pontryagin, V.G. Boltyanskii, E.F. Gamkrelidze, and E.F. Mishchenko, *The Mathematical Theory of Optimal Processes*. New York: Interscience, 1965.
- [23] M. Bavaro, "Metodi di controllo per robot intrinsecamente sicuri," M.S. thesis, Università di Pisa, Pisa, Italy, 2003.
- [24] M.W. Spong, "Modeling and control of elastic joint robots," *ASME J. Dynamic Syst., Measurement, and Control*, vol. 109, no. 4, pp. 310–319, 1987.
- [25] A. De Luca and P. Lucibello, "A general algorithm for dynamic feedback linearization of robots with elastic joints," in *IEEE Int. Conf. Robot. and Automat.*, Leuven, Belgium, 1998, pp. 504–510.
- [26] R. Kelly, R. Ortega, A. Ailon, and A. Loria, "Global regulation of flexible joints robots using approximate differentiation," *IEEE Trans. Automat. Contr.*, vol. 39, no. 6, pp. 1222–1224, 1994.
- [27] L. Lanari, P. Sicard, and J.T. Wen, "Trajectory tracking of flexible joint robots: A passivity approach," in *Proc. Euro. Control Conf.*, Groningen, Holland, 1993.
- [28] A. Konno and M. Uchiyama, "Vibration suppression control of spatial flexible manipulators," *Control Eng. Practice*, vol. 3, no. 9, pp. 1315–1321, 1995.
- [29] A. De Luca, "Feedforward/feedback laws for the control of flexible robots," in *Proc. IEEE Int. Conf. Robot. and Automat.*, San Francisco, CA, 2000, pp. 233–240.
- [30] G.A. Pratt and M. Williamson, "Series elastics actuators," in *Proc. IEEE/RSJ Int. Conf. Intell. Robots and Syst.*, Pittsburgh, PA, 1995, pp. 399–406.
- [31] M. Okada and Y. Nakamura, "Development of the cybernetic shoulder—A three-DOF mechanism that imitates biological shoulder

- motion,” in *Proc. IEEE/RSJ Int. Conf. Intell. Robots and Syst.*, Korea, October 1999, pp. 453–548.
- [32] J.L. Nevins and D.E. Whitney, “The force vector assembler concept,” in *Proc. 1st Int. Symp. Robotics and Manipulators*, Udine, Italy, 1973.
- [33] K.F. Laurin-Kovitz, J.E. Colgate, and S.D.R. Carnes, “Design of programmable passive impedance,” in *Proc. IEEE Int. Conf. Robot. and Automat.*, 1991, pp. 1476–1481.
- [34] T. Morita and S. Sugano, “Design and development of a new robot joint using a mechanical impedance adjuster,” in *Proc. IEEE Int. Conf. Robot. and Automat.*, 1995, pp. 2469–2475.
- [35] N. Takesue, G. Zang, J. Furusho, and M. Sakaguchi, “Precise position control of robot arms using a homogeneous ER fluid,” *IEEE Contr. Syst. Mag.*, pp. 55–61, vol. 19, Apr. 1999.
- [36] M. Suzuki, D.M. Shiller, P.L. Gribble, and D.J. Ostry, “Relationship between contraction, movement kinematics and phasic muscle activity in single joint arm movement,” *Experimental Brain Res.*, vol. 140, no. 2, pp. 171–181, 2001.
- [37] D-73230 Kirchheim Teck (Germany) HEXAGON Industriesoftware GmbH, Stiegelstrasse 8. Available: <http://www.hexagon.de/index.htm>
- [38] D.G. Caldwell, G.A. Medrano-Cerda, and M.J. Goodwin, “Control of pneumatic muscle actuators,” *IEEE Contr. Syst. J.*, vol. 15, no. 1, pp. 40–48, Feb. 1995.
- [39] C.P. Chou and B. Hannaford, “Measurement and modeling of artificial muscles,” *IEEE Trans. Robot. Automat.*, pp. 90–102, 1996.
- [40] N-C. Park, H-W. Park, H-S. Yang, and Y-P. Park, “Robust position and force control of two d.o.f. flexible manipulators with artificial muscle,” in *Proc. Int. Conf. Motion and Vibration Contr.*, Zurich, Switzerland, 1998.
- [41] London N1 1LX UK Shadow Robot Company Ltd., 251 Liverpool Road. Available: <http://www.shadow.org.uk/products/airmuscles.html>
- [42] J.M. Hollerbach, I.M. Hunter, and J. Ballentyne, “A comparative analysis of actuator technologies for robotics,” in *The Robotics Review 2*, O. Khatib, J.J. Craig, and T. Lozano-Perez, Eds. Cambridge, MA: MIT Press, 1991.
- [43] Y. Bar-Cohen, “Electroactive polymers as artificial muscles: Capabilities, potentials and challenges,” in *Handbook on Biomimetics*, Yoshihito Osada (Ed.). NTS Inc., 2000, ch. 8.
- [44] B. Siciliano and L. Villani, “An inverse kinematics algorithm for interaction control of a flexible arm with a compliant surface,” *Contr. Eng. Practice*, vol. 9, pp. 191–198, 2001.
- [45] B. Brogliato and R. Lozano, “Correction to adaptive control of robot manipulators with flexible joints,” *IEEE Trans. Automat. Contr.*, vol. AC-41, no. 6, pp. 920–922, 1996.
- [46] M. Kawato, “Internal models for motor control and trajectory planning,” in *Current Opinion in Neurobiology*. Oxford: Elsevier, vol. 9, 1999, pp. 718–727.
- [47] R. Shadmehr and F.A. Mussa-Ivaldi, “Geometric structure of the adaptive controller of the human arm,” Tech. Rep. AI Memo 1437, MIT, Boston, MA, July 1993.

**Antonio Bicchi** received the “Laurea” degree in mechanical engineering from the University of Pisa in 1984 and the Doctoral degree from the University of Bologna in 1989. After a postdoctoral fellowship at the Artificial Intelligence Lab, Massachusetts Institute of Technology, he joined the Faculty of Engineering at the University of Pisa in 1990. He is a full professor of systems theory and robotics in the Department of Electrical Systems and Automation (DSEA) of the University of Pisa. He currently serves as the director of the Interdepartmental Research Center “E. Piaggio” of the University of Pisa, where he has been leading the Automation and Robotics group since 1990. His main research interests are in robotics, in the fields of dextrous manipulation and haptics (including force/torque and tactile sensing, and sensory control), in the dynamics, kinematics, and control of complex mechanical systems, including autonomous vehicles and automotive systems; and more generally in the theory and control of nonlinear systems, including nonholonomic and hybrid (logic/dynamic, symbol/signal) systems. He has published more than 170 papers on international journals, books, and refereed conferences. He is a Distinguished Lecturer of the IEEE Robotics and Automation Society. He also serves as chairman of the IEEE Control Systems Society Technical Committee on Manufacturing, Automation, and Robotics Control (MARC).

**Giovanni Tonietti** received the Laurea Degree in computer science in 2001 from the Faculty of Engineering, University of Pisa. Currently, he is a Ph.D. student in robotics, automation, and bioengineering at the Centro Interdipartimentale di Ricerca “E. Piaggio” and at the Dipartimento di Sistemi Elettrici and Automazione, at the University of Pisa. His research is mainly involved in the study, design, and control of safe and performant actuation systems for robotics.

**Address for Correspondence:** Antonio Bicchi, Centro Interdipartimentale di Ricerca “E. Piaggio,” Università di Pisa, Pisa, Italy. E-mail: [bicchi@ing.unipi.it](mailto:bicchi@ing.unipi.it).